RSC Advances

PAPER

View Article Online
View Journal | View Issue

Cite this: *RSC Adv.*, 2024, **14**, 19206

High-efficiency removal of As(III) from groundwater using siderite as the iron source in the electrocoagulation process†

Haitao Yu,[a] Junfeng Li, *[ab] Wenying Qu,[ab] Wenhuai Wang[ab] and Jiankang Wang[ab]

Electrocoagulation technology, due to its simplicity and ease of operation, is often considered for treating arsenic-contaminated groundwater. However, challenges such as anode wear have hindered its development and application. This study aims to develop a siderite-filled anode electrocoagulation system for efficient removal of As(III) and investigate its effectiveness. The impact of operational parameters on the removal rate of As(III) was analyzed through single-factor tests, and the stability and superiority of the device were evaluated. The response surface methodology was employed to analyze the interactions between various factors and determine the optimal operational parameters by integrating data from these tests. Under conditions where the removal rate of As reached 99.3 ± 0.37%, with an initial concentration of As(III) at 400 μg L^{-1}, current intensity at 30 mA, initial solution pH value at 7, and Na_2SO_4 concentration at 10 mM. The flocculant used was subjected to characterization analysis to examine its structure, morphology, and elemental composition under these optimal operational parameters. The oxidation pathway for As(III) within this system relies on integrated results from direct electrolysis as well as $^{\bullet}O_2^-$, $^{\bullet}OH$, and Fe(IV) mediated oxidation processes. The elimination of arsenic encompasses two fundamental mechanisms: firstly, the direct adsorption of As(III) by highly adsorbent flocculants like γ-FeOOH and magnetite (Fe_3O_4); secondly, the oxidation of As(III) into As(V), followed by its reaction with siderite or other compounds to generate a dual coordination complex or iron arsenate, thus expediting its eradication. The anodic electrocoagulation system employing siderite as a filler exhibits remarkable efficiency and cost-effectiveness, while ensuring exceptional stability, thereby providing robust theoretical underpinnings for the application of electrocoagulation technology in arsenic removal.

Received 11th April 2024
Accepted 11th June 2024

DOI: 10.1039/d4ra02716g

rsc.li/rsc-advances

1 Introduction

Arsenic (As) is a metallic substance that poses a carcinogenic risk to human health.[1–4] It occurs naturally in both organic and inorganic forms.[4] In contrast to organic arsenic, the toxicity of inorganic arsenic makes it a significant concern for scientific research.[5] Human activities often contribute to high concentrations of arsenic in the environment, resulting from excessive mining and smelting, untreated discharge of industrial wastewater, as well as widespread use of arsenic and its compounds.[6] Consequently, water bodies are increasingly affected by severe arsenic pollution, posing a substantial threat to global populations.[7,8]

Compared to As(V), As(III) exhibits higher toxicity and mobility, making the removal of As(III) from arsenic-contaminated groundwater a pressing issue for societal development.[9,10] Various water treatment techniques, including coagulation,[11,12] adsorption,[13] biological process[14] ion exchange,[15,16] and membrane separation[17,18] have been proposed for remediating arsenic-contaminated groundwater. However, these technologies face practical challenges due to their high cost, maintenance requirements, and potential for secondary pollution. Electrocoagulation technology was initially reported by the United Kingdom in 1889 for sewage treatment and was later adopted in the United States in 1946.[19,20] Nevertheless, limitations such as significant capital investment and inadequate electrode replacement hinder its practical application.[21,22] Flores[23] demonstrated a total arsenic removal rate of 92% using an aluminum electrode-based continuous flow electrocoagulation system at pH 7.5 with a velocity of 1.8 cm s^{-1} and current density of 6 mA cm^{-2}. Similarly to electrocoagulation methods, Ghurye and Clifford[24] propose that adsorption following chemical oxidation is a more effective approach for arsenic removal. However, in most cases of

[a]College of Water Conservancy and Architectural Engineering, Shihezi University, Shihezi, 832000, Xinjiang, PR China. E-mail: ljfshz@126.com
[b]Key Laboratory of Cold and Arid Regions Eco-Hydraulic Engineering of Xinjiang Production & Construction Corps, Shihezi, 832000, Xinjiang, PR China

† Electronic supplementary information (ESI) available. See DOI: https://doi.org/10.1039/d4ra02716g

electrocoagulation processes utilizing sacrificial anodes for contaminant removals lead to frequent anodic replacements during practical applications; improper electrode replacement often disrupts device operation.

Siderite, a widely distributed iron mineral with excellent adsorption properties, predominantly consists of ferrous carbonate.[25] It plays a pivotal role in environmental pollution control due to its remarkable attributes including cost-effectiveness, high adsorption capacity, eco-friendliness, stability, and recyclability.[26] The surface activity of siderite enables the efficient adsorption of heavy metal ions and radioactive elements while catalyzing the degradation of organic pollutants.[27,28] Moreover, it forms complexes with water contaminants for purification purposes and facilitates REDOX reactions. Despite previous investigations on siderite's efficacy in removing water arsenate and arsenate through adsorption processes,[29,30] limited studies have explored its potential as an iron source for electrocoagulation reactions.

In summary, arsenic contamination in natural water bodies poses a threat to human health. The existing treatment technology for arsenic-contaminated water needs to be acknowledged and addressed systematically. While previous studies have explored the removal of arsenic and arsenate from water through electrocoagulation, limited research has utilized iron minerals as the iron source for the electrocoagulation reaction, leaving the effect and mechanism of As(III) on arsenic in water unclear. Although using siderite-filled anodes can address issues such as anode loss and difficult electrode replacement encountered in traditional electrocoagulation processes, there is a lack of investigation into its application for treating arsenic-containing water. In conclusion, this paper conducts experimental research on a siderite-filled anode electrocoagulation system to optimize electrocoagulation technology for removing As(III) from water while effectively addressing limitations associated with traditional methods. This study provides new insights into treating As(III) and heavy metals in water.

This study aims to establish an electrocoagulation system with a siderite-filled anode for efficient treatment of As(III) pollutants in water, based on the electrocoagulation water treatment technology. The specific research objectives are to:

(1) Construct the siderite-filled anode electrocoagulation system and determine factors that influence As(III) removal.

(2) Optimize the operational parameters for the removal of As(III) from groundwater through a response surface method (RSM).

(3) Elucidate the oxidation pathway and removal mechanism of As(III) through comprehensive characterization techniques including scanning electron microscopy (SEM), X-ray fluorescence analysis (XRF), Fourier transform infrared spectroscopy (FTIR), X-ray diffraction (XRD), and X-ray photoelectron spectroscopy (XPS). These analyses provided insights into the morphology, structure, and elemental composition of the flocculated products. Subsequently, a series of chemical tests was conducted to investigate the oxidation path of As(III) in the electrocoagulation process. Finally, the oxidation removal mechanism of As(III) in the electrocoagulation water treatment process was clarified.

In general, this study can better solve the problem that the anodes are not easy to replace due to the click loss of electrocoagulation technology, and provide theoretical guidance and practical reference for the treatment of arsenic contaminated groundwater by electrocoagulation.

2 Materials and experimental

2.1. Chemicals and equipment

The chemical reagents utilized in this study are presented in Table S1.† H_2SO_4 and NaOH were employed for sample pH adjustment during experimentation. The instruments and models employed for testing purposes are detailed in Table S2.†

2.2. Electrocoagulation process

In this study, natural siderite was incorporated into the conventional electrocoagulation process as the iron source for the electrocoagulation reaction, and a siderite-filled anode electrocoagulation system was developed.

The test apparatus described herein involves overflow of the reaction mixture from the upper reactor into the lower beaker, followed by recirculation of the reaction liquid back to the upper reactor *via* a peristaltic pump, thus establishing a closed-loop circulation system. The specific configuration of the experimental setup is depicted in Fig. 1. The upper reactor consists of a cylindrical plexiglass column with a volume of 350 mL. Hollow cylinders made of titanium ruthenium mesh are positioned within this reactor as anodes, while natural siderite particles serve as both fillers inside these anodes and sources of iron for facilitating electrocoagulation reactions. Two pure aluminum electrode plates are symmetrically arranged on either side of each anode (with respect to its center) to function as cathodes for promoting electrocoagulation reactions. A cylindrical plexiglass column with a volume of 250 mL is connected beneath this reactor to collect overflow liquid from above; subsequently, under peristaltic pump action, solution from this lower plexiglass column is returned to bottom region of upper reactor to achieve arsenic removal from solution samples being treated hereunder experimentally conducted conditions.

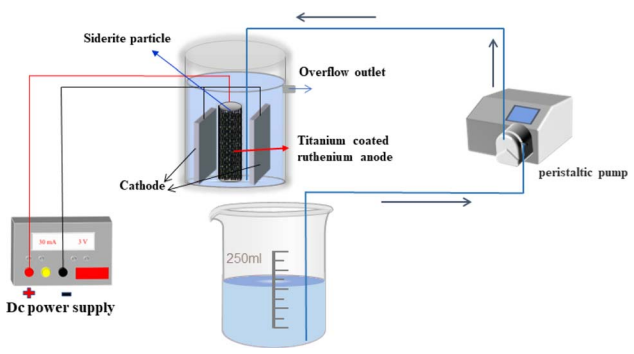

Fig. 1 Schematic representation of an electrocoagulation reaction apparatus.

2.3. Design of experiment

In order to investigate the impact of various operational parameters on the removal efficiency of As(III), different factors were analyzed while keeping other influencing variables constant. The specific experimental design is as follows: the initial As(III) ranges explored in single-factor experiments were 200, 400, 600, 800, 1000 μg L^{-1}; current intensity ranges of 10, 20, 30, 40, 50 mA; the initial pH range is 3, 5, 7, 9, 11; electrolyte (Na_2SO_4) concentration ranges of 5, 10, 15, 20 mM; peristaltic pump cycle rate range is 0, 50, 100, 150 mL min^{-1}. The effect of phosphoric acid concentration 0, 1, 5, 15 mg L^{-1}, silicate concentration 0, 5, 10, 50 mg L^{-1} and humic acid concentration 0, 1, 5, 10 mg L^{-1} on the removal rate of As(III). The run time of each experiment was keeping 60 minutes. Instantaneous sampling technology was used to collect samples every 1, 3, 5, 10, 15, 30, 45, and 60 minutes for testing, and samples were filtered through a 0.45 μm filter to determine the concentrations of As(III) and total arsenic. To minimize experimental errors, each test was repeated three times.

To investigate the long-term operational stability and arsenic removal efficiency of the systems in removing As(III) from water and better simulate its application in actual operations, cyclic experiments were conducted. Before each set of experiments, fresh simulated groundwater was injected into the reactor, and the experiment was repeated six times, with no replacement of the siderite particles inside the anode. Although the stability of long-term repeated operation of the experimental device cannot be obtained by conducting six cycle tests, it is sufficient to show that the device has a relative sense of operation stability. Lastly, to investigate the system's ability to remove arsenic from real groundwater, the ability of the systems to remove arsenic from real groundwater under optimal operating conditions was explored. The purpose of this study was to explore the process of removing As(III) from water by adding siderite particles to the anode to dissolve and release iron sources, so the effect of cathodic dissolution on electrocoagulation reaction was not considered.

2.4. Method of analysis

The total iron concentration in the solution was determined using the phenanthroline spectrophotometric method. The absorbance was measured at a wavelength of 510 nm using a purple spectrophotometer. The concentrations of As(III) and total arsenic in the solution were determined using atomic fluorescence spectrophotometry. Electron spin resonance (ESR) was used to detect $^{\cdot}OH$ and $^{\cdot}O_2^-$ in the system. Scanning electron microscopy (SEM) was used to observe the surface morphology of siderite and flocs. X-ray fluorescence spectroscopy (XRF) was used to analyze the chemical composition of siderite and flocs. X-ray diffraction (XRD) was used to analyze the properties and structure of flocs. Fourier-transform infrared spectroscopy (FTIR) was used to distinguish the chemical structure of flocs. X-ray photoelectron spectroscopy (XPS) was used to determine the valence states of As and Fe in the precipitate.

Arsenic removal rate (Re%) was calculated by eqn (1):[31]

$$\mathrm{Re} = \frac{C_0 - C_i}{C_0} \times 100\% \quad (1)$$

where C_0 is the concentration of arsenic before the reaction, C_i is the concentration of arsenic after the reaction, μg L^{-1}.

2.5. Data processing

The Design expert 10.0.3 software for data analysis was utilized to conduct multiple regression fitting on the test data, with *A* representing current intensity, *B* denoting initial pH, and *C* indicating peristaltic pump cycle rate. The actual arsenic removal rate was considered as the response variable for performing multiple regression fitting on these parameters while analyzing the interaction among different factors to obtain the predicted optimal operating parameters.

3 Results and discussion

3.1. Influence of various factors on As(III) removal efficiency

3.1.1 Initial As(III) concentration. Fig. 2a examines the effects of different initial arsenic concentrations on arsenic removal performance. As can be seen from the figure, arsenic removal rates exceed 98%, and at initial arsenic concentrations of 200–600 μg L^{-1}, arsenic removal rates are 99.6 ± 0.75%, 99.3 ± 0.37%, and 99.11 ± 0.54%, respectively. The residual arsenic content of the solution in the discharge water was all reduced to less than 10 μg L^{-1}. In the case of an initial arsenic concentration of 800–1000 μg L^{-1}, the residual arsenic concentrations in the solution are 14.98 μg L^{-1} and 16.80 μg L^{-1}, respectively, at which point the remaining arsenic is As(V). The reason for the high arsenic concentration in the effluent may be due to the fact that the dissolved iron source is not sufficient to adsorb the arsenic concentration under the assumption that the amount of iron source released by the system is constant in the case of a constant flow size. Therefore, when treating water with a high concentration of arsenic, there will be a situation where the flocculant cannot completely adsorb arsenic within a fixed time.

3.1.2 Initial pH. The effects of pHs of 3, 5, 7, 9 and 11 on arsenic removal performance were investigated in Fig. 2b. When pH < 7, the removal rate of arsenic increases with the increase of pH. At pH > 7, the removal rate of arsenic decreases as pH increases. At different pH, the removal rate of arsenic can be ordered as pH = 7 > pH = 5 > pH = 9 > pH = 3 > pH = 11. At pH = 7, the removal rate of arsenic reached the maximum of 99.3 ± 0.37%. This may be because the iron hydroxide produced in the electrocoagulation reaction process will mainly exist in the form of fibritite, its conductive point is about pH = 7.0, at pH = 7, the electrostatic attraction between As(V) and Fe_2O_3.

At pH < 7.0, As(V) and the surface of iron hydroxide are positively charged, resulting in the adsorption of iron hydroxide for As(V) is reduced due to electrostatic repulsion. Although the removal rate of As(V) is relatively slow when the pH is too low or too high, the removal rate is 97.35 ± 1.75% at pH = 5, and 96.78 ± 1.53% at pH = 9, and the final removal rate of arsenic is roughly the same. This shows that the electrocoagulation reaction can work effectively over a wide pH range, and in theory, enough iron hydroxide can be produced to completely

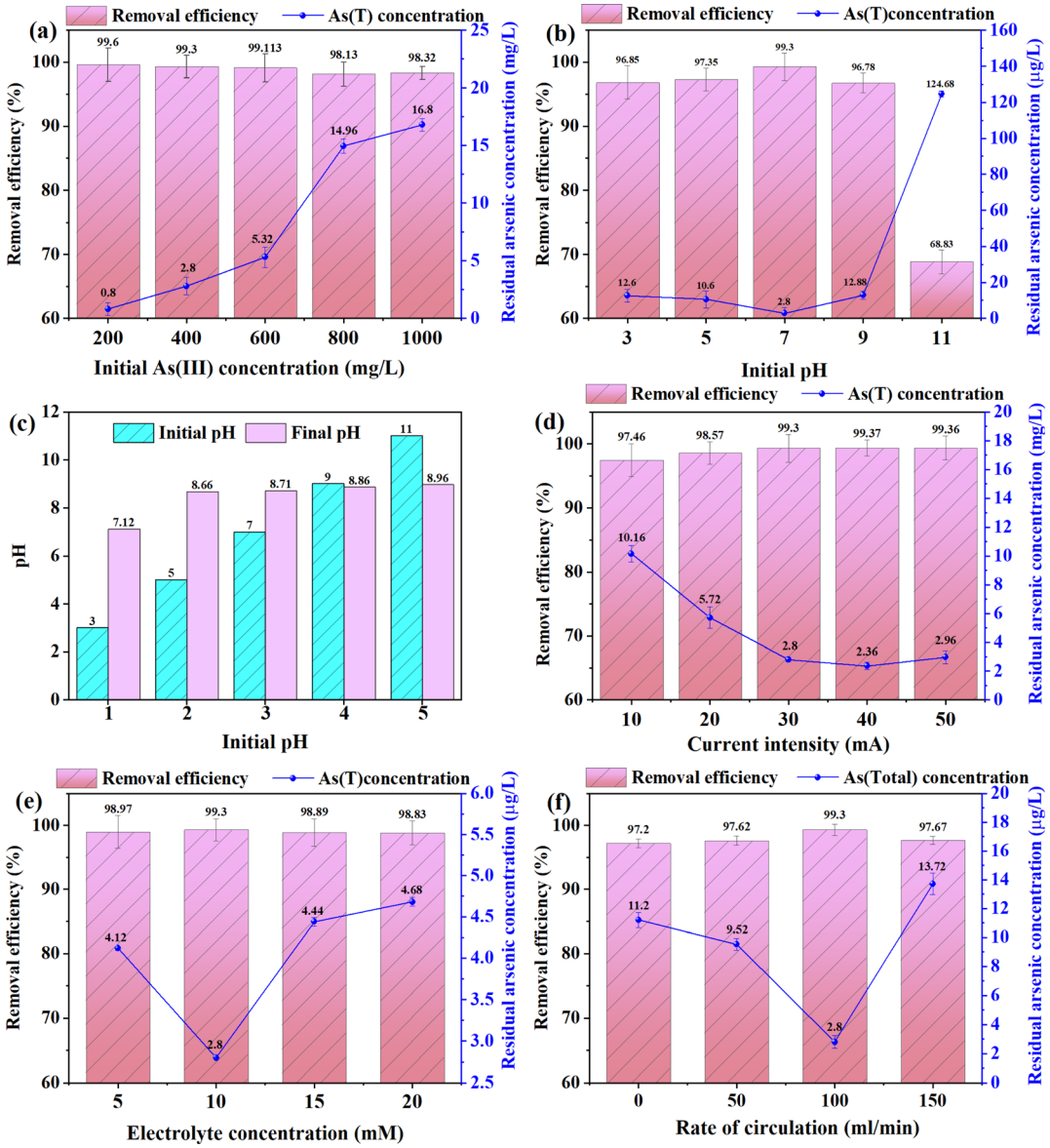

Fig. 2 Effect of (a) initial As(III) concentration; (b) initial pH; (c) pH changes before and after reaction; (d) Na_2SO_4 concentration; (e) intensity of current; and (f) rate of circulation on As(III) removal.

remove arsenic from the solution. However, at pH 9.0–11.0, the removal rates of arsenic are 96.78 ± 1.53% and 68.83 ± 1.85%, respectively. The reason for the decrease in the removal rate of arsenic may be that the proportion of $Fe(OH)_3$ produced at this time decreases, and some iron ions generate $Fe(OH)_4$,[32] which leads to a sharp decline in the removal rate of arsenic at this time. In addition, as shown in Fig. 2c, the effluent pH of the solution will stabilize in a weakly alkaline range after the reaction at different pH, which indicates that the electrocoagulation reaction can effectively adjust the effluent pH of the solution.[33,34]

3.1.3 Current intensity. Fig. 2d shows the effect of different current intensities on arsenic removal performance. The removal rate of arsenic increases with the increase of the current intensity, and the removal rate of arsenic is 97.46 ± 0.56% and 98.57 ± 0.75% when the current intensity is 10 mA and 20 mA, respectively. When the current intensity is 30 mA, the removal rate of arsenic is 99.3 ± 0.37%, when the current intensity is 30 mA, the reaction basically reached equilibrium, at this time the concentration of arsenic in the solution (2.80 μg L^{-1}) is much lower than 10 μg L^{-1}. When the current intensity is 40 mA and 50 mA, the removal rate of arsenic is 99.37 ± 0.23% and 99.36 ± 0.86%, respectively. After 30 mA, the improvement of As(III) removal rate was negligible with the increase of current intensity. The increase of current intensity has little effect on As(III) removal rate. Considering the effect of removal rate and economy, the current intensity of 30 mA was adopted in all subsequent experiments.

3.1.4 Initial Na_2SO_4 concentration. The electrolyte concentration often determines the conductivity of the solution, and adding a certain amount of Na_2SO_4 to the solution will improve the conductivity of the solution. As shown in Fig. 2e,

the removal rates at Na_2SO_4 concentrations of 5, 10, 15 and 20 mM were 98.97 ± 0.56%, 99.3 ± 0.37%, 98.89 ± 0.54% and 98.83 ± 0.85%, respectively. With the increase of electrolyte concentration, the removal rate of As(III) showed a trend of first increasing and then decreasing. However, the overall removal rate of arsenic did not change significantly. The highest removal rate was observed when the concentration of Na_2SO_4 was 10 mM. An electrolyte is a substance that speeds up sediment formation and stabilizes the interaction between the reactants.[35] The concentration of the electrolyte tends to affect the charge distribution between the ions in the electrocoagulation reaction and thus affect the electrocoagulation result. The presence of electrolytes can effectively reduce the surface tension of the solution, making the reaction easier to carry out. The increase of electrolyte concentration will destroy the anode surface and the passivation film formed on the siderite surface, thus promoting the electrocoagulation reaction. However, when the electrolyte concentration was higher than 10 mM, the removal rate of As(III) did not improve significantly. Too much electrolyte may inhibit other interionic reactions in the water, but as can be seen from the figure, the effect is small. It showed that the supporting electrolyte addition had no significant effect on As removal efficiency and energy consumption. Therefore, the optimal Na_2SO_4 concentration used in this experiment is 10 mM.

3.1.5 The influence of peristaltic pump circulation rate. In the electrocoagulation experiment, the oxidation reaction of Fe(II) largely depends on the availability of dissolved oxygen. In order to explore the effect of dissolved oxygen on the removal rate of arsenic, the experiment uses peristaltic pump as the linker, which changes the free dripping of the solution under different peristaltic pump rates, thus affecting the performance of the electrocoagulation reaction. As shown in Fig. 2f, with the increase of peristaltic pump rate, the removal rate of arsenic in the solution showed a trend of first increasing and then decreasing. When the peristaltic pump circulation rate was 0, 50, 100 and 150 mL min^{-1}, the removal rate was 78.97 ± 0.56%, 97.02 ± 0.64%, 99.33 ± 0.37% and 97.67 ± 0.52%, respectively. Therefore, it can be determined that when the peristaltic pump rate is 100 mL min^{-1}, the removal rate of arsenic reaches the best. In the electrocoagulation reaction, increasing the contact with the air can promote the electrocoagulation reaction.[36,37] In the electrocoagulation reaction, the gas produced by the reaction may participate in the reaction and promote the electrocoagulation reaction, thus accelerating the electrocoagulation efficiency. Contact with gas can affect the progress of electrocoagulation reaction.

3.1.6 The influence of phosphoric acid concentration. Under different phosphate concentrations, the removal rate of As(III) decreased with the increase of phosphate ion concentration, indicating that phosphate has obvious inhibitory effect on the removal of arsenic. As shown in Fig. 3a, at different phosphate concentrations, the final removal rates of arsenic were 99.30 ± 1.65%, 90.38 ± 0.96%, 72.83 ± 1.51%, 55.85 ± 1.67%, respectively. Arsenic in nature mainly reacts with iron, manganese, aluminum and so on to form oxides or hydroxides, which exist in sediments or soil in water bodies. In addition, arsenic and phosphorus belong to Group V of the periodic table of chemical elements, have similar chemical properties, and therefore have similar chemical transformation processes.

The coexistence of ions in water may promote or inhibit the adsorption of arsenic by the flocs produced by the electrocoagulation reaction. Generally, the content of phosphorus in water is higher than that of arsenic in water. Previous studies have shown that competitive adsorption of phosphorus and arsenic often occurs in soil,[38] which also leads to a great reduction of the maximum adsorption capacity of the adsorbent for arsenic in the treatment process.[39] Phosphate is considered to be the most competitive ion with arsenic in water. The deprotonated oxygen-containing anion formed by phosphate in water occupies the adsorption site on the surface of iron oxide, thus inhibiting the adsorption behavior of arsenic. In the electrocoagulation reaction, As(III) is usually oxidized to As(V) by electrolysis and oxidation of active free radicals. The chemical structure dissociation constant of phosphate (PO_4^{3-}) is similar to that of arsenate (AsO_4^{3-}). Therefore, in the electrocoagulation system filled with siderite anode, when there are phosphoric acid and arsenate at the same time, there is bound to be competitive adsorption on the surface of iron oxide, which will also lead to the reduction of arsenic removal rate.

3.1.7 The influence of the concentration of silicate. In order to investigate the effect of different concentrations of silicates on the removal rate of As(III) in electrocoagulation system filled with siderite anode. The results are shown in Fig. 3b, and the results show that the silicate has an inhibitory effect on the removal of As(III). With the increase of the concentration of silicate ion in water, the removal rate of As will continue to decrease. However, compared with phosphoric acid, silicate has less influence on As(III) removal rate in water. The removal rates of arsenic were 99.3 ± 1.86%, 98.83 ± 2.03%, 97.68 ± 0.65% and 88.45 ± 2.44%, respectively, at different concentrations of silicate.

The removal of arsenic in electrocoagulation system filled with siderite anode, in which the anions come from silicates and phosphates. The concentration of these two anions can reach 10–70 mg L^{-1} (measured in SiO_2), which is much higher than the arsenic concentration in groundwater, so they will adsorb and participate in the treatment process of arsenic in groundwater. First of all, both phosphates and silicates have an inhibitory effect on the removal of arsenic, mainly because they can form a chemical reaction similar to that of phosphate and silicates with iron oxides with As(V), leading to a reduction in the adsorption site, thereby reducing the removal rate of arsenic. In addition, phosphates and silicates will also prevent the formation of iron hydroxide flocs through oxidation with Fe(II). This finding has important theoretical guiding significance and practical application value for the effective removal of arsenic from groundwater.

3.1.8 Influence of humic acid concentration. Humic acid is a range of organic materials accumulated by the remains of plants and animals, mainly plants, through decomposition and transformation by microorganisms, and a series of chemical changes on the Earth's surface. The main organic matter in natural drinking water is humic acid, the content of humic acid

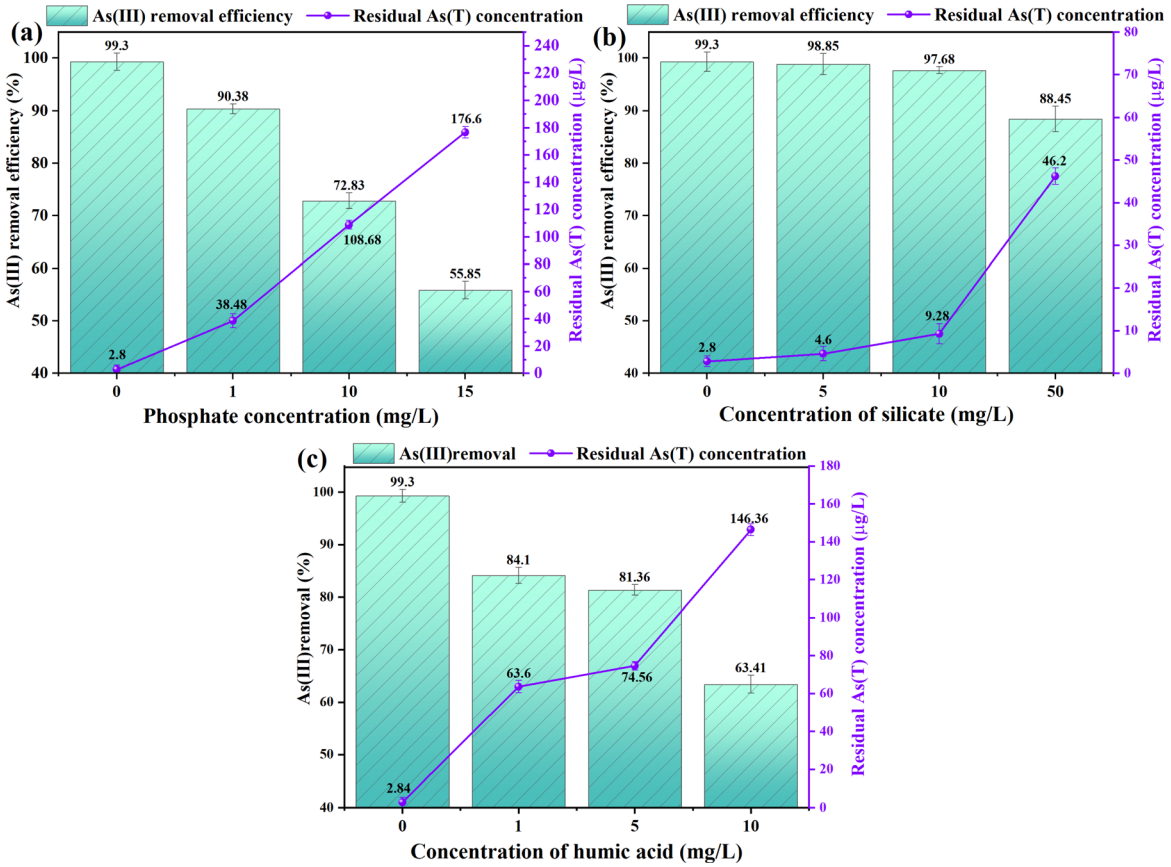

Fig. 3 Effect of (a) phosphate concentration; (b) concentration of silicate; (c) concentration of humic acid on As(III) removal.

in the general water source is about 10 mg L^{-1}, the higher the content, the worse the water quality. Humic acid due to the existence of a large number of free radicals on its surface such as carboxyl, hydroxyl, carbonyl and other active free radicals, its physiological activity makes humic acid cause harm to the cone. Humic acid is electronegative in water, easy to complex with trace elements in water, especially heavy metals, to produce more toxic substances, and can also lead to water-insoluble compounds become easily soluble, so that its migration ability in water is improved.

When the initial concentration of As(III) in water is 400 μg L^{-1}, the current intensity is 30 mA, the pH is 7, the electrolyte (Na_2SO_4) concentration is 10 mM, and the peristaltic pump rate is 100 mL min^{-1}, the effects of different concentrations of humic acid (0, 1, 5, 10 mg L^{-1}) in electrocoagulation system filled with siderite anode on the removal rate of arsenic were investigated. As shown in Fig. 3c, humic acid at different concentrations had obvious inhibition on arsenic removal. The removal rates of As(III) under different humic acid concentrations were 99.30 ± 1.21%, 84.10 ± 1.52%, 81.36 ± 0.98%, 63.41 ± 1.69%. The removal rate of arsenic was greatly reduced in the electrocoagulation reaction of humic acid, which may be due to the competition between humic acid and As(V) at the surface adsorption points, and the formation of soluble and colloidal Fe(III)-HA complexes inhibited the precipitation of iron oxides/hydroxides.

3.2. The response surface method was used to optimize the test parameters

3.2.1 The establishment of response surface model. The experimental Design[40] and test results obtained by the response surface method are shown in Table S3.† Multiple regression fitting is performed on the test data by using the Design expert 10.0.3 data analysis software. The current intensity, initial pH and peristaltic pump cycle rate are set as A, B and C, respectively, and the actual arsenic removal rate is taken as the response value to perform multiple regression fitting on the parameters. The coefficient and significance test results of the regression model are shown in Table S4.† The quadratic multinomial regression model is obtained, as shown in eqn (2):

$$Y = 98.75 + 2.23\ 4.4 \times B \times C + 1.22 + 2.62 \times AB - AC + 6.09 \times 5.84 \times BC - 12.84 \times A^2 - 13.9 \times B^2 - 13.89 \times C^2 \quad (2)$$

After the regression model is obtained, further regression analysis is carried out on the actual arsenic removal rate model and regression coefficient. The results are shown in Table S4.† From Table S4,† it can be seen that $P < 0.001$ (extremely significant) and its missing item $P = 0.0848 > 0.05$ (insignificant) of the regression model, indicating a good degree of fitting of the model and the corresponding regression value of the regression equation can be predicted. At the same time, the regression coefficient of the model $R^2 = 0.9892$, and the

adjusted R^2 = 0.9754 (greater than 0.8000), indicating that 97.54% of the data can be explained by the model, indicating that the reliability of the equation is high.

As shown in Fig. S1,† the actual and predicted values of each factor on the removal rate of arsenic are almost distributed in a straight line with the results of the response values and the test values, the actual values of the 17 groups of tests are close to the response values, indicating a good fit. Residual analysis is used to obtain the difference between the test value and the response value, and can be used to investigate the reliability of the model and data. As shown in Fig. S2(a),† the number of values corresponding to the residual and response values is randomly distributed around the zero line, and the floating range of the residual value is within ±6, indicating a high degree of fit and small error. As can be seen from the residual value based on the predicted removal rate of arsenic in Fig. S2(b),† if the residual value and the normal distribution value are basically in a straight line, the confidence degree of the data is high, indicating that the residual follows the normal distribution. In summary, it indicates that the model has good fitting and rationality, and can be used to optimize the process conditions of arsenic removal rate.

3.2.2 Analysis and verification of response surface model. Then, according to the regression equation, the shape of response surface curve and contour map were investigated to analyze the effects of current intensity, initial pH and peristaltic pump cycle rate on the actual As(III) removal rate. The response surface curves and contours can well reflect the interaction between the independent variables. By observing the steepness of the slope of the response surface graph, we can determine the degree of influence between the two response variables on the response value. The steeper the response surface graph, the more obvious the interaction between the two response variables. The effects of current intensity (*A*), initial pH (*B*) and cycle rate (*C*) on the actual arsenic removal rate can be obtained by analyzing Fig. 4a and b, b and e, and c and f.

The effect of the interaction between current intensity and pH on the actual arsenic removal rate is shown in Fig. 4a. On the *AB* interaction surface, the slope of the actual arsenic removal rate increases first and then decreases with the change of current intensity and pH. When the current intensity is 25–35 mA and pH is about 6–8, the actual arsenic removal rate is the highest. The response surface diagram is also consistent with the results of ANOVA in Table S4.†

The influence of the interaction between current intensity and cycle rate on the actual arsenic removal rate is shown in Fig. 4b. In *AC* interaction surface, the slope of the actual arsenic removal rate increases first and then decreases with the increase of current intensity; when the current intensity is low, the slope of the actual arsenic removal rate increases first and then gently with the increase of cycle rate; when the current intensity is high, the slope of the actual arsenic removal rate increases first and then gently. The slope of the actual arsenic removal rate increases first and then decreases with the increase of the cycling rate, which indicates that there is a significant interaction between the current intensity and the cycling rate. When the current intensity is 25–35 mA and the cycle rate is about 70–130 mL min^{-1}, the actual arsenic removal rate is the highest. The curve diagram is also consistent with the results of variance analysis in Table S3.†

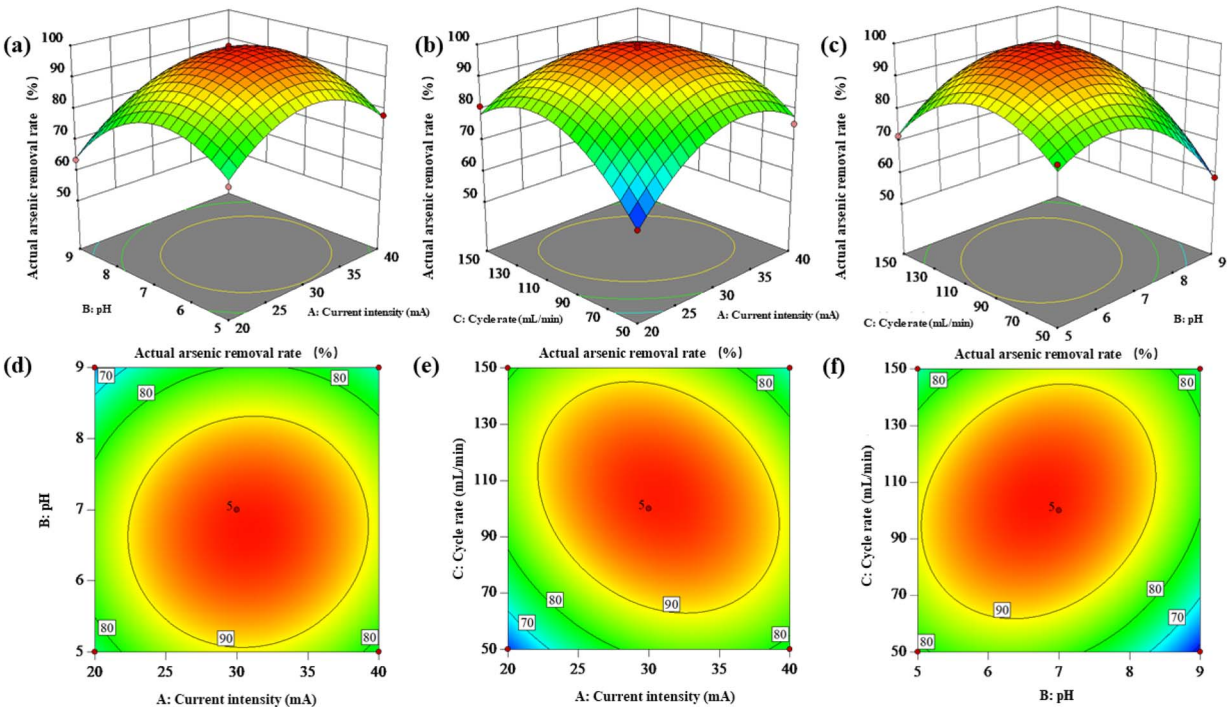

Fig. 4 Response surface plot (a–c) and contour lines (d–f) of the combined effect of intensity of current, initial pH, and rate of circulation on As(III) removal.

The interaction of pH and circulation rate has an impact on the actual arsenic removal rate as shown in Fig. 4c. In the BC interaction surface, with the increase of circulation rate, the actual arsenic removal rate increases first and then decreases; when the circulation rate is low, the slope of the actual arsenic removal rate increases first and then becomes gentle with the increase of pH; when the circulation rate is high, the actual arsenic removal rate increases first and then becomes gentle. The slope of the actual arsenic removal rate increases first and then decreases with the increase of the cycling rate, indicating that pH and the cycling rate have a strong interaction. When pH is 6–8 and the cycling rate is about 70–130 mL min^{-1}, the actual arsenic removal rate is the largest. The plots were also consistent with the ANOVA results.

After the experiment, according to the obtained regression equation model, the optimal operating conditions for the prediction were as follows: current intensity is 30.682 mA, pH is 6.710, cycle rate is 102.449 mL min^{-1}. According to the actual conditions of the experiment, the conditions are revised to current intensity is 30 mA, initial pH is 7, cycle rate is 100 mL min^{-1}. Under the optimal conditions, three parallel tests determined that the actual removal rate of arsenic was 99.332 ± 0.568%, which was within 5% of the predicted removal rate of 99.205%, confirming the good correlation between the predicted value and the experimental value, indicating that the optimal operating parameters optimized by the response surface method were reasonable.

3.3. Characterization of flocs

3.3.1 SEM and XRF analysis. The surface morphology and element content analysis of the flocs are shown in Fig. 5a and b. The surface of the flocs is irregular particles with relatively loose particle distribution and porous structure, which is conducive to the adsorption of arsenic. XRF analysis is usually used to determine the composition and content of the group elements in the floc. It can be seen from Fig. 5c and d that XRF elemental analysis indicates that the oxides that may exist in the floc are Fe_3O_2, Al_2O_3, As_2O_3, *etc.* The main elements in the floc are iron, oxygen, carbon, arsenic, *etc.* After inspection, the content of the main elements is 64.50% oxygen, 18.90% iron, 12.40% carbon and 4.20% arsenic respectively. According to the scanning electron microscope image, arsenic was uniformly distributed in the floc, and the proportion of iron content was high, indicating that a large number of iron flocculants could be produced in the reaction to adsorb arsenic. It can be concluded that the removal of arsenic is mainly based on the adsorption of iron precipitates. In addition, the oxygen content contained in the floc is high, it can be inferred that some floc exists in the form of oxides or hydroxides.

3.3.2 FTIR Analysis. Subsequently, FTIR analysis is performed on the floc in the wave number range of 500 cm^{-1} to 4000 cm^{-1} to obtain the infrared spectrum of the floc absorption. As shown in Fig. 6a, a new characteristic peak appears at the wavelength of 562.63, which is caused by Fe–O vibration of Fe_3O_4 minerals in the iron-containing floc.[41] The wave number peak at 1124.29 is due to the asymmetric stretching of Fe–C–O, indicating a chemical bond formed by the reaction between the arsenic and the iron floc in solution. In addition, 818 to 1128 cm^{-1} is the vibration absorption band of fibritite, and 585 to 632 cm^{-1} may be the stretching vibration absorption band of As(III)–O.[42] There are O–H bonds in the floc, and it is speculated that there may be hydrogen bonds and OH connections in the floc. The characteristic peaks at 1638.70 and 3460.10 cm^{-1} indicate that there are hydrogen bonds in the product to be connected with OH. The characteristic peak at 2965.50 cm^{-1} indicates the presence of C–H bond in the product. The results show that there are many strong peaks in the electrocoagulation system filled with siderite anode, which is sufficient to indicate the presence of pure crystal components in the flocs, which is consistent with the results obtained by XRF analysis.

3.3.3 XRD analysis. The XRD pattern of the sediment phase analysis is shown in Fig. 6b. The weak diffraction peak and relatively dim diffraction peak in the flocculant directly detected at room temperature indicate that the crystallinity of the flocculant is low. Through analysis, it is assumed that the crystallization peak of arsenic is the main peak, but the peak is not

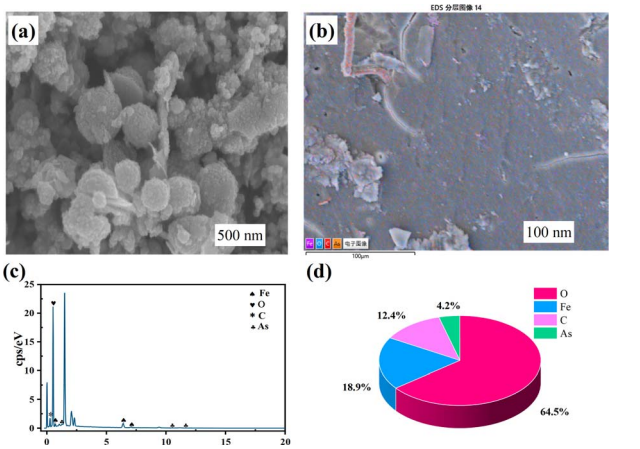

Fig. 5 SEM (a and b) and XRF (c and d) characterization of flocculants.

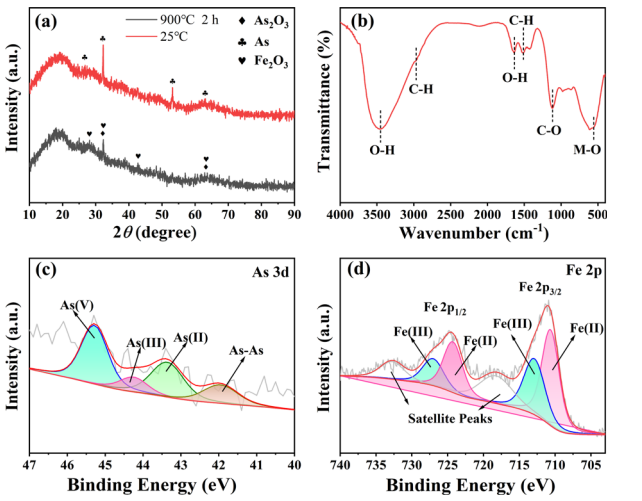

Fig. 6 Flocculants characterization: (a) the XRD analysis; (b) FTIR analyses; (c). XPS spectrum of Fe 2p; (d). XPS spectrum of As 3d.

obvious. The characteristic diffraction peak at $2\theta = 56.728°$ corresponds to γ-FeOOH (PDF# 76–2301). Subsequently, after calcination at 900 °C for 2 h, it was found that the diffraction peak at this time was still not obvious, which may be due to the temperature at this time still did not reach the conditions for the production of crystallization of iron elements, at this time the crystallization peak of Fe_2O_3 mainly exists in the floc, the peak is still not obvious, so it is concluded that the floc is more stable, not easy to crystallization. Therefore, it can be concluded that the electrocoagulation system filled with siderite anode has a strong adsorption capacity for arsenic pollutants during the sedimentation process.

3.3.4 XPS analysis. X-ray photoelectron spectroscopy (XPS) is a commonly used material characterization method, which can accurately analyze the elements and their valence states on the surface of materials. It can be used to analyze the surface of micron films or other types of materials, and has good theoretical application effect. In this study, this technique was used to analyze the floc produced by the electrocoagulation reaction.

The analysis of the valence states of arsenic and iron in the sediment with XPS, as shown in Fig. 6c, can be found in the Fe 2p spectrum of XPS, which consists of Fe 2p and Fe $2p_{2/3}$ original Fe $2p_{1/2}$ spectra. Consisting of 6 peaks, respectively, formed by two asymmetric peaks centered on the binding energies of 710.64 eV and 724.27 eV in the figure.[43,44] In addition, it can be inferred by comparison that the material with a peak Fe $2P_{3/2}$ of 711.20 eV may be magnetite (Fe_3O_4), ferritic hematite (γ-FeOOH), or hematite (α-Fe_2O_3)[45] and the peak at 712.30 eV and 726.00 eV is Fe(II).[46] The peaks at 710.20 eV and 723.90 eV belong to As(III),[44] and the peaks at 719.40 eV and 732.60 eV correspond to satellite peaks.[43] In the As 3d image of XPS Fig. 6d, it can be seen that most of the arsenic is in the form of As(III), so it can be concluded that most of the As(III) is oxidized to As(V).

3.4. Oxidation of As(III)

In order to explore the oxidation path of As(III) in the electrocoagulation reaction, the contribution of each free radical to the electrocoagulation reaction is determined by the electrolytic direct oxidation (without adding siderite), the oxidation of arsenic after adding siderite, and the possible active free radicals (˙OH, Fe(IV)) in the quenching reaction process.

As shown in Fig. 7, the oxidation path of As(III) under the optimal operating parameters is explored, and the removal rate of arsenic in the solution after 10 min is shown under different conditions (direct oxidation by electrolysis, oxidation of arsenic after adding siderite, quenching of ˙OH, and oxidation of arsenic after quenching of Fe(IV)).

Under the optimal operating parameters, the direct reaction in the electrocoagulation device with siderite filled anode without siderite was found that the oxidation rate of arsenic reached 78% within 10 min. The results show that the direct oxidation of electrode has great contribution in the electrochemical reaction. Then siderite was added to continue the reaction, and it was found that the oxidation rate of arsenic at 10 min was 87.79%, which indicated that siderite was also involved in the oxidation of arsenic. Then methanol was added

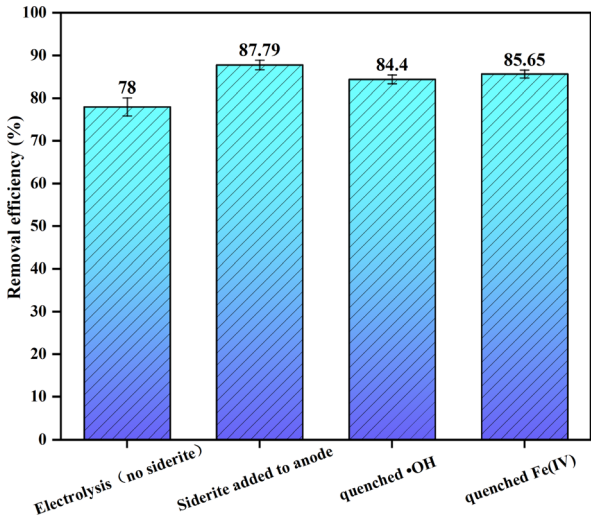

Fig. 7 Oxidation rate of As(III) at 10 min after addition of quencher.

to the solution as the quenching agent of ˙OH, and it was found that the oxidation rate of arsenic was reduced by 3.39% within 10 min. When dimethyl sulfone was added as Fe(IV) quenching agent, the oxidation rate of arsenic was reduced by 4.14%. This indicates that ˙OH and participate in the oxidation of As(III).

In addition, the electrocoagulation system filled with siderite anode is powered by a peristaltic pump, which increases the oxygen content in the reaction liquid by overflow. After O_2 is introduced into the system, Fe(II) will be rapidly oxidized. According to the above experimental phenomena, it is speculated that the electrocoagulation system filled with siderite anode is very likely to occur electrofenton reaction.[47,48] However, the mechanism of the electrofenton reaction is complex and controversial. In this study, ˙OH and $^{\cdot}O_2^-$ in the solution were detected by electron spin resonance spectroscopy. The results were shown in Fig. S3 and S4,† and four characteristic peaks were found in the solution respectively. This also confirmed the existence of ˙OH and $^{\cdot}O_2^-$ in the solution to oxidize As(III).

It was also proved that ˙OH was formed during the reaction in the electrocoagulation system filled with siderite anode. This can be interpreted as: due to the presence of O_2, will oxidize eqn (3) rapidly. Similarly, the production of ˙OH will be accompanied by the production of $^{\cdot}O_2^-$ (ref. 49) and H_2O_2 (ref. 50) eqn (4). Under the condition of pH = 7, the formation of Fe(IV)[51] in the electrocoagulation reaction is also very likely to exist, As shown in eqn (5) and (6), during the reaction process, the oxidizing agent generated will oxidize As(III) in the system to As(V)[52] eqn (7)–(10).

$$Fe^{2+} + O_2 \rightarrow Fe^{3+} + {}^{\cdot}O_2^- \quad (3)$$

$$Fe^{2+} + {}^{\cdot}O_2^- + 2H^+ \rightarrow Fe^{3+} + H_2O_2 \quad (4)$$

$$Fe^{2+} + H_2O_2 \rightarrow Fe^{3+} + {}^{\cdot}OH + OH^- \quad (5)$$

$$Fe^{2+} + H_2O_2 \rightarrow Fe^{4+} + 2OH^- \quad (6)$$

$$As^{3+} - 2e^- \rightarrow As^{5+} \quad (7)$$

$$As^{3+} + 2^{\cdot}O_2^{-} + 2H^{+} \rightarrow As^{5+} + 2HO_2^{-} \quad (8)$$

$$As^{3+} + 2^{\cdot}OH \rightarrow As^{5+} + 2OH- \quad (9)$$

$$2Fe^{4+} + As^{3+} \rightarrow 2Fe^{3+} + As^{5+} \quad (10)$$

In summary, the oxidation of As(III) in electrocoagulation system filled with siderite anode is the comprehensive result of direct electrolysis of electrode, $^{\cdot}O_2^{-}$, $^{\cdot}OH$ and oxidation of Fe(IV).

3.5. The removal mechanism of As(III)

In the electrocoagulation system filled with siderite anode, the introduction of siderite replaces the supply of iron ions in the previous electrocoagulation process using iron as anode. Therefore, it is not difficult to surmise that the presence of iron ions in the reaction system will have a certain impact on the reaction effect. Because of its high catalytic activity and affinity for arsenic, iron-based materials usually oxidize As(III) to As(V) rapidly in heterogeneous Fenton systems. As(V) is then removed from the water by adsorption and industrial precipitation on the surface. Therefore, the oxidation path of As(III) is discussed in detail here.

In this paper, there may also be oxidation of As(III) due to the release of iron ions from siderite.[53] Therefore, in order to explore whether there is such a phenomenon, we have explored the oxidation pathway of As(III) in the previous article. In the results of exploration, we can find that Fe(IV) is produced in the system, which does have a certain impact on the oxidation of As(III).[54] Therefore, the existence of siderite has also been confirmed in the system occurred a class - Fenton reaction, Fe(II) under the action of oxygen reaction to produce Fe(III), at the same time the generation of $^{\cdot}O_2^{-}$, $^{\cdot}O_2^{-}$ may react As(III) oxidation to As(V); in addition, in the process of system reaction, the system will continue to release Fe(II), the generated Fe(II) and the previous generation of $^{\cdot}O_2^{-}$ and electrolysis of H^{+} continue to react to generate H_2O_2; the Fe(II) in the system will continue to undergo a reaction with H_2O_2 to produce Fe(IV).[55] This may result in an Fe(IV) reaction path in the system. Therefore, Fe(II) in the system will be partially converted to Fe(IV) and participate in the oxidation of As(III). Secondly, when H_2O_2 exists in the system, part of Fe(II) will be oxidized to Fe(III) under its action, and in this reaction process, there will be the generation of $^{\cdot}OH$. $^{\cdot}OH$ will also react with As(III) to oxidize it to As(V). In order to verify the existence of the above content, the quenching test and the detection of the presence of $^{\cdot}OH$ were carried out previously, which confirmed the correctness of the above statement. Therefore, we can conclude that there are four oxidation paths of Fe(II) in the system: Fe(II) reacts with oxygen, Fe(II) reacts with $^{\cdot}O_2^{-}$ and H^{+}, reacts with Fe(II) reacts with H_2O_2 to produce Fe(III), and reacts with Fe(II) and H_2O_2 to produce Fe (IV). In this process, the $^{\cdot}O_2^{-}$, $^{\cdot}OH$, Fe(IV) generated in the system will continue to react with As(III) in the system, thus oxidizing part of the system As(III) to As(V). Lakshmanan *et al.* believe that in ferroelectric flocculation system, low voltage direct current is applied to the low carbon steel plate immersed in the electrolyte to promote the oxidation of Fe(0) on the iron anode to Fe(II), and the reduction of H_2O to H_2 (g) on the iron cathode.[56] *In situ* formed Fe(II) is further oxidized by dissolved O_2 in bulk solution to form an insoluble Fe(III) (oxygenated) oxide in addition, reactive intermediates (*i.e.* O_2 oxidation of Fe(II) to produce $^{\cdot}OH$, and $^{\cdot}O_2^{-}$, and Fe(IV)) oxidizes As(III) to As(V), which adsorbs more readily than As(III). This is also consistent with the results obtained in this study.

As(III) removal mechanism is shown in the Fig. 8. Therefore, in the electrocoagulation system filled with siderite anode, the oxidation path of As(III) can be divided into the following four types: (1) electrolytic direct oxidation; (2) indirect oxidation of $^{\cdot}O_2^{-}$; (3) indirect oxidation of $^{\cdot}OH$; and (4) indirect oxidation of Fe(IV). Through a series of characterization analysis of the floc, the main mechanism of removing As(III) in water by the electrocoagulation system filled with siderite anode is obtained as follows: under the stimulation of the current, siderite releases a large amount of Fe(II), and Fe(II) will then be oxidized by the system into Fe(III) substances, that is, ferritic hematite (γ-FeOOH), magnetite (Fe_3O_4) and $Fe(OH)_3$. Part of As(III) in water will be oxidized into As(V) through the above several ways, because the pH is neutral conditions, so As(III) in water will exist in the form of H_3AsO_3 and H_2AsO, As(V) will exist in the form of $H_2AsO_4^{-}$, $HAsO_4^{2-}$ and AsO_4^{3-}. As(III) is oxidized to As(V), $FeAsO_4$ complex is easily formed and removed by precipitation. γ-FeOOH and $Fe(OH)_3$ produced by oxidation of Fe(II) will accelerate the settlement of suspended matter in solution. The iron flocculant produced by the reaction is flocculated and precipitated together with the arsenate in the water, thus achieving the purpose of removing arsenic.

Under the action of the anode, siderite steadily releases Fe(II), which is further oxidized to form γ-FeOOH. Since the solution has both As(III) and As(V) in the process of reaction, it is speculated that the electrocoagulation reaction mainly has two mechanisms to remove As(III) : first, As(III) in the electrocoagulation system in the electrocoagulation system filled with siderite anode is directly removed by the flocculant with strong adsorption capacity such as ferritic hematite (γ-FeOOH), magnetite (Fe_3O_4), and the second is As(III) is oxidized to As(V), and then the formation of bicoordination complex or iron arsenate with fiber iron ore and is removed.

3.6. Stability test of the device

For mature water treatment technology, an important parameter that can be recognized is the long-term stability of the water treatment device. Compared with the traditional electrocoagulation process, which uses the iron electrode as the iron source directly to provide the iron source for the electrocoagulation reaction, this study adopts the method of siderite releasing iron ions under the electrochemical action of the anode to continuously provide the iron source for the electrocoagulation reaction. There may be insufficient iron source supply. Therefore, it is very necessary to determine the stability of repeated operation of the electrocoagulation device through tests.

The stability of iron flocculant produced by electrolysis of siderite is the key factor of arsenic removal in electrocoagulation system filled with siderite anode during long-term

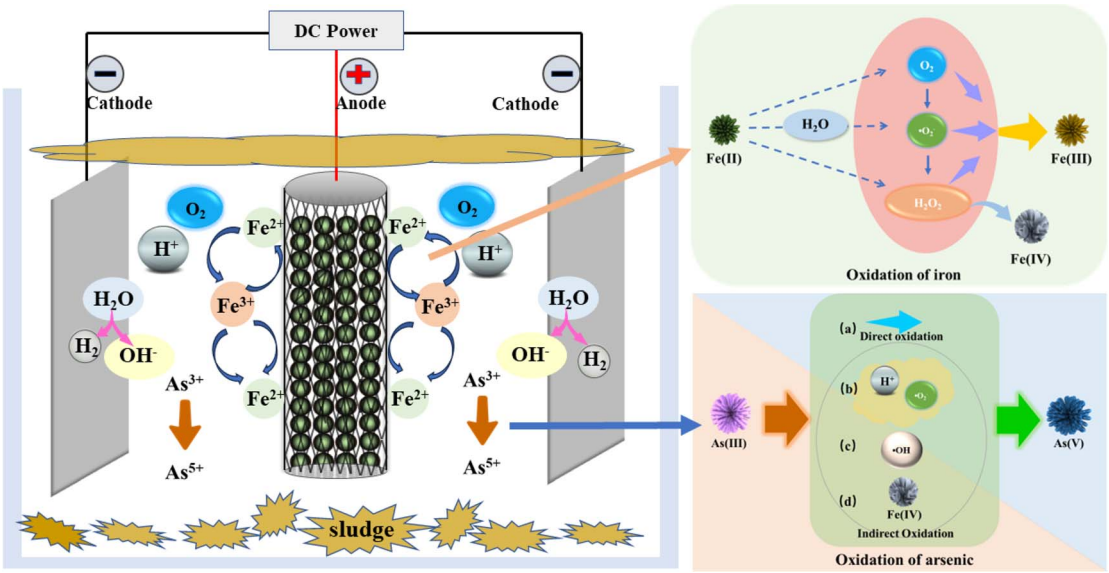

Fig. 8 Mechanism of the siderite electrocoagulation process in removing As(III).

operation. In order to accurately evaluate the influence of this factor, the cycle experiment was carried out under the optimal operating parameters, and the siderite was not replaced during the cycle experiment. Due to the limitation of the iron content of siderite itself, it was found in the pre-experiment that with the increase of the number of tests, the content of iron ions visible to the naked eye in the solution decreased significantly, and the concentration of iron ions decreased after about 3–5 times, so the number of cyclic experiments was determined to be 6 groups. As shown in Fig. 9a, as the number of cycles increased, the removal rate of arsenic decreased from 99.30 ± 0.37% to 98.60 ± 0.45%, but overall the removal rate of arsenic was relatively stable. After 6 cycles, the residual concentration of arsenic in the effluent was 5.60 ± 1.8 μg L^{-1}, which was in line with the concentration range stipulated by the World Health Organization.

After a series of cyclic tests, the system demonstrated its capability to maintain a high arsenic removal efficiency, largely attributed to the precise determination of optimal operating parameters. Additionally, the study found that the introduction of oxygen (O_2) into the system *via* overflow contributed to enhanced arsenic removal efficiency.[49] Experimental comparisons between th system and an electrocoagulation (EC) system without overflow were conducted, the experimental setup (no peristaltic pump) as shown in Fig. S5a.† With the results depicted in Fig. S5b† showing a significant increase in arsenic removal rate under overflow conditions. Specifically, the residual arsenic concentrations in the effluent were 2.8 ± 1.48 μg L^{-1} and 14.17 ± 2.85 μg L^{-1} for the overflow and no-overflow conditions, respectively. Fig. S5c† examined the changes in As(V) concentration over time, revealing an initial increase followed by a decrease, peaking at around 10 minutes. In the system, the peak concentration of As(V) occurred slightly earlier and was slightly higher compared to the no-overflow condition. This suggests that overflow accelerates the oxidation of As(III) to As(V) and also promotes the oxidation of Fe(II), thereby

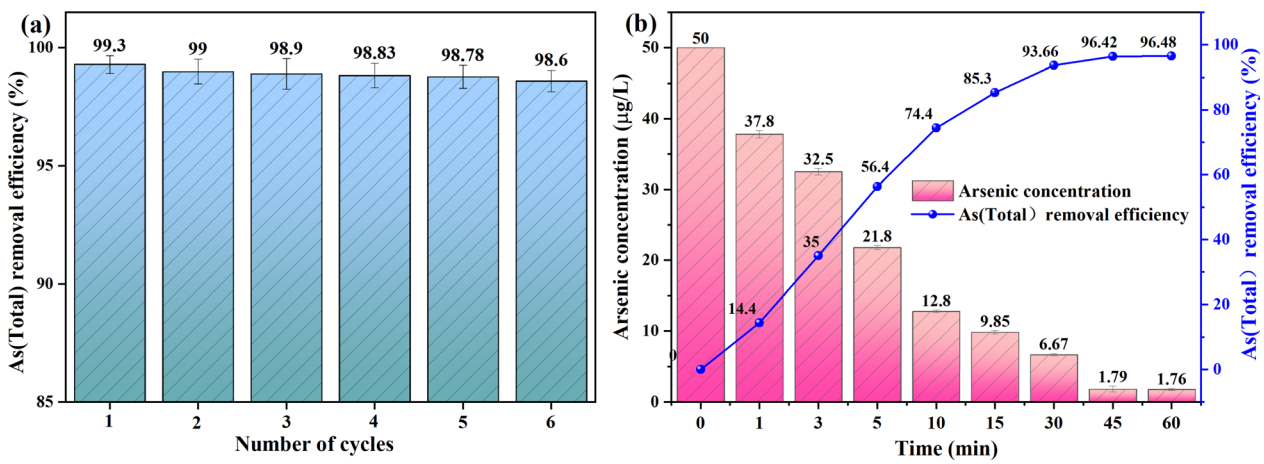

Fig. 9 Siderite electrocoagulation process actual operation test: (a) six cycles of experiments; (b) the treatment of actual groundwater.

hastening the formation of coagulants and enhancing the removal of arsenic.

3.7. Removal test of As(III) in actual groundwater

In order to evaluate the removal efficiency of As(III) in actual water by the electrocoagulation system filled with siderite anode, the initial pH of the water sample was 6.70–8.50 and the conductivity was 1739 μS cm^{-1} based on the actual local groundwater. After detecting the arsenic content in the actual groundwater, a certain amount of As(III) was added to obtain the As(III) exceeded the standard groundwater based on the actual groundwater, of which the initial As(III) concentration was 50 μg L^{-1}.

In this study, real groundwater samples with an As(III) concentration of 50 μg L^{-1} were treated under optimal conditions to validate the practical application potential of the electrocoagulation system filled with siderite anode in treating high-arsenic groundwater. The experimental results indicated that the system achieved an arsenic removal efficiency of 96.48% ± 0.27%. The valence state of arsenic in the treated water was converted to As(V), with the concentration reduced to 1.76 ± 0.14 μg L^{-1}, significantly below the World Health Organization's standard of 10 μg L^{-1}. These findings demonstrate the effectiveness of the system in removing excessive arsenic from groundwater. Compared to the removal rate of 99.3% under laboratory conditions, there was a slight decrease in the removal efficiency in the field application, which could be attributed to the lower initial concentration of arsenic in the actual groundwater and the influence of other ions present in the groundwater,[57] such as phosphate and silicate ions.[42] Nevertheless, the system maintained a high level of arsenic removal from groundwater, demonstrating its ability to effectively remove arsenic from actual groundwater sources.

4 Conclusions

The present study investigates the incorporation of natural siderite into an electrocoagulation system for enhanced removal efficiency and mechanism elucidation of As(III). The specific findings are as follows:

(1) The operation parameters are optimized using the response surface method based on a single factor experiment. the optimal conditions for the system were determined: initial As(III) concentration of 400 μg L^{-1}, current intensity of 30 mA, pH = 7, and Na_2SO_4 concentration of 10 mM, under which the removal rate of arsenic can reach 99.3% ± 0.37%.

(2) The oxidation of As(III) involves direct electrode oxidation to produce reactive oxidants, followed by coagulation and adsorption removal. The pathways for As(III) oxidation include direct electrolytic oxidation and reactive oxygen species oxidation(possibly $^{\bullet}O_2^-$, $^{\bullet}OH$, and Fe(IV)).

(3) After six consecutive cycles of testing, the arsenic removal rate decreased slightly from 99.30% ± 0.37% to 98.60% ± 0.45%, showing overall stability in arsenic removal efficiency.

(4) When treating real groundwater with high arsenic content, the removal rate reached 96.48% ± 0.27%, and the effluent arsenic concentration was 1.76 ± 0.14 μg L^{-1}, significantly below the World Health Organization's standard of 10 μg L^{-1}. This indicates that the system can effectively remove excessive arsenic from groundwater.

In summary, this study successfully developed an environmentally friendly, highly efficient, and stable method for removing arsenic from groundwater, providing innovative ideas and theoretical support for the application of electrocoagulation technology in treating arsenic-containing groundwater. This device provides a reference and technical support for removing As(III) from water in remote areas. It offers important experimental evidence and theoretical guidance for the field of water treatment technology, having a profound impact on advancing and improving existing water treatment methods.

Data availability

The data supporting this article have been included as part of the ESI.†

Author contributions

H. T. Yu: conceptualization, methodology, writing—original draft preparation; J. F. Li: validation, supervision, project administration, funding acquisition; W. H. Wang: validation, data curation; H. T. Yu and W. H. Wang: software, data curation; J. K. Wang and W. Y. Qu: visualization, investigation; J. F. Li and W. Y. Qu: funding acquisition, project administration.

Conflicts of interest

The authors declare that they have no conflict of interest.

Acknowledgements

Financial support from the National Natural Science Foundation of China (52260002, 42107414, 52300214), the Youth Innovation and Cultivation Talent Project of Shihezi University (CXFZ202201, CXPY202201), the Annual Youth Doctoral Program of Xinjiang Uyghur Autonomous Region 'Tianchi Elite' Introduction Plan (CZ002302, CZ002305), High Level Talent Research Launch Project of Shihezi University (RCZK202316, RCZK202321) are gratefully acknowledged.

References

1 N. Dutta and A. Gupta, *J. Water Process Eng.*, 2022, **49**, 103013.
2 L. Weerasundara, Y.-S. Ok and J. Bundschuh, *Environ. Pollut.*, 2021, **268**, 115668.
3 D. S. Babu and P. V. Nidheesh, *Chem. Eng. Commun.*, 2021, **208**, 389–410.
4 A. Basu, D. Saha, R. Saha, T. Ghosh and B. Saha, *Res. Chem. Intermed.*, 2014, **40**, 447–485.
5 P. Mondal, C. B. Majumder and B. Mohanty, *J. Hazard. Mater.*, 2006, **137**, 464–479.

6 Rakhmania, H. Kamyab, M. A. Yuzir, N. Abdullah, L. M. Quan, F. A. Riyadi and R. Marzouki, *Sustainability*, 2022, **14**, 1985.
7 L. Rodriguez-Lado, G. Sun, M. Berg, Q. Zhang, H. Xue, Q. Zheng and C. A. Johnson, *Science*, 2013, **341**, 866–868.
8 Y. Li, Q. Zhang, D. Wang, B. Yang, X. Zhi, S. Fan, M. He, Q. Zheng and G. Sun, *Fresenius Environ. Bull.*, 2015, **24**, 3057–3062.
9 S. Gong, J. Yang, W. Zhou, X. Liu and D. Wang, *J. Cleaner Prod.*, 2023, **428**, 139533.
10 S. R. Kanel, T. K. Das, R. S. Varma, S. Kurwadkar, S. Chakraborty, T. P. Joshi, A. N. Bezbaruah and M. N. Nadagouda, *ACS Environ. Au*, 2023, **3**(3), 135–152.
11 S. Song, A. Lopez-Valdivieso, D. J. Hernandez-Campos, C. Peng, M. G. Monroy-Fernandez and I. Razo-Soto, *Water Res.*, 2006, **40**, 364–372.
12 M. I. Litter, M. E. Morgada and J. Bundschuh, *Environ. Pollut.*, 2010, **158**, 1105–1118.
13 D. E. Giles, M. Mohapatra, T. B. Issa, S. Anand and P. Singh, *J. Environ. Manage.*, 2011, **92**, 3011–3022.
14 S. R. Manoj, C. Karthik, K. Kadirvelu, P. I. Arulselvi, T. Shanmugasundaram, B. Bruno and M. Rajkumar, *J. Environ. Manage.*, 2020, **254**, 14.
15 B. An, Q. Q. Liang and D. Y. Zhao, *Water Res.*, 2011, **45**, 1961–1972.
16 B. F. Urbano, B. L. Rivas, F. Martinez and S. D. Alexandratos, *React. Funct. Polym.*, 2012, **72**, 642–649.
17 I. A. Katsoyiannis and A. I. Zouboulis, *Rev. Environ. Health*, 2006, **21**, 25–41.
18 E. Gunes and Z. B. Gonder, *J. Environ. Manage.*, 2021, **294**, 14.
19 O. Sahu, B. Mazumdar and P. K. Chaudhari, *Environ. Sci. Pollut. Res.*, 2014, **21**, 2397–2413.
20 E. A. Vik, D. A. Carlson, A. S. Eikum and E. T. Gjessing, *Water Res.*, 1984, **18**, 1355–1360.
21 M. Eyvaz, M. Kirlaroglu, T. S. Aktas and E. Yuksel, *Chem. Eng. J.*, 2009, **153**, 16–22.
22 C. A. Basha, S. J. Selvi, E. Ramasamy and S. Chellammal, *Chem. Eng. J.*, 2008, **141**, 89–98.
23 O. J. Flores, J. L. Nava and G. Carreno, *Int. J. Electrochem. Sci.*, 2014, **9**, 6658–6667.
24 G. Ghurye, D. Clifford and J. Am, *Water Works Assoc.*, 2004, **96**, 84–96.
25 H. Sun, J. Yao, B. Ma, T. S. Knudsen and C. Yuan, *Sci. Total Environ.*, 2024, **914**, 169922.
26 G.-Q. Li, C. Wang, Y. Zhang, H. Wan, M. Dou and H. Xu, *Water Reuse*, 2022, **12**, 319–331.
27 H. Liu, X. Li, X. Zhang, F. Coulon and C. Wang, *Chemosphere*, 2023, **337**, 139404.
28 F. Sun, T. Chen, H. Liu, X. Zou, P. Zhai, Z. Chu, D. Shu, H. Wang and D. Chen, *Sci. Total Environ.*, 2021, **784**, 147117.
29 S. Y. Lee, B. Chang, Y. Kim, H. Jang and Y. J. Lee, *J. Colloid Interface Sci.*, 2022, **613**, 499–514.
30 H. Guo, D. Stüben and Z. Berner, *J. Colloid Interface Sci.*, 2007, **315**, 47–53.
31 M. Chen, H. Hu, M. Chen, C. Wang, Q. Wang, C. Zeng, Q. Shi, W. Song, X. Li and Q. Zhang, *J. Hazard. Mater.*, 2023, **441**, 129884.
32 D. S. Babu, P. V. Nidheesh and M. S. Kumar, *Sep. Sci. Technol.*, 2021, **56**, 184–193.
33 T. Honda, K. Murase, T. Hirato and Y. Awakura, *J. Appl. Electrochem.*, 1998, **28**, 617–622.
34 Y. Lei, B. Song, R. D. van der Weijden, M. Saakes and C. J. N. Buisman, *Environ. Sci. Technol.*, 2017, **51**, 11156–11164.
35 X. G. Meng, S. Bang and G. P. Korfiatis, *Water Res.*, 2000, **34**, 1255–1261.
36 Y. Si, G. Li and F. Zhang, *Environ. Sci. Technol.*, 2017, **4**, 71–75.
37 J. H. Brunsting and E. A. McBean, *J. Contam. Hydrol.*, 2014, **159**, 20–35.
38 S. P. Funk, L. Duffin, Y. H. He, C. McMullen, C. X. Sun, N. Utting, J. W. Martin, G. G. Goss and D. S. Alessi, *J. Contam. Hydrol.*, 2019, **221**, 50–57.
39 C. M. Su and R. W. Puls, *Environ. Sci. Technol.*, 2001, **35**, 4562–4568.
40 K. Yaghmaeian, S. S. Martinez, M. Hoseini and H. Amiri, *Desalin. Water Treat.*, 2016, **57**, 27827–27833.
41 J. S. Zhou, H. H. Song, L. L. Ma and X. H. Chen, *RSC Adv.*, 2011, **1**, 782–791.
42 S. Goldberg and C. T. Johnston, *J. Colloid Interface Sci.*, 2001, **234**, 204–216.
43 H. Sun, G. Z. Zhu, X. T. Xu, M. Liao, Y. Y. Li, M. Angell, M. Gu, Y. M. Zhu, W. H. Hung, J. C. Li, Y. Kuang, Y. T. Meng, M. C. Lin, H. S. Peng and H. J. Dai, *Nat. Commun.*, 2019, **10**, 11.
44 C. Ma, P. F. Yuan, S. Y. Jia, Y. Q. Liu, X. J. Zhang, S. Hou, H. X. Zhang and Z. G. He, *Waste Manage.*, 2019, **83**, 23–32.
45 J. N. Fiedor, W. D. Bostick, R. J. Jarabek and J. Farrell, *Environ. Sci. Technol.*, 1998, **32**, 1466–1473.
46 J. Wang, Z. F. Cao, H. S. Ren, C. Yu, S. Wang, L. Q. Li and H. Zhong, *Appl. Surf. Sci.*, 2020, **500**, 10.
47 S. J. Hug and O. Leupin, *Environ. Sci. Technol.*, 2003, **37**, 2734–2742.
48 D. Syam Babu, K. Vijay, P. V. Nidheesh and M. Suresh Kumar, *Sustain. Energy Technol. Assessments*, 2021, **47**, 101476.
49 D.-h. Kim, A. D. Bokare, M. s. Koo and W. Choi, *Environ. Sci. Technol.*, 2015, **49**, 3506–3513.
50 W. Ren, D. Tang, M. Huang, J. Sun and K. Lv, *J. Hazard. Mater.*, 2018, **350**, 88–97.
51 L. Li, C. M. van Genuchten, S. E. A. Addy, J. Yao, N. Gao and A. J. Gadgil, *Environ. Sci. Technol.*, 2012, **46**, 12038–12045.
52 J. A. G. Gomes, P. Daida, M. Kesmez, M. Weir, H. Moreno, J. R. Parga, G. Irwin, H. McWhinney, T. Grady, E. Peterson and D. L. Cocke, *J. Hazard. Mater.*, 2007, **139**, 220–231.
53 Q.-w. Wang, X.-l. Yan, M.-j. Ma, B.-s. Li, Z.-r. Li and Q.-z. Li, *Trans. Nonferrous Met. Soc. China*, 2022, **32**, 4139–4155.
54 T. Demirel, F. K. Ozmen, Y. Yavuz and A. S. Koparal, *Appl. Water Sci.*, 2022, **12**, 138.
55 W. H. Holl, *Environ. Geochem. Health*, 2010, **32**, 287–290.
56 D. Lakshmanan, D. A. Clifford and G. Samanta, *Water Res.*, 2010, **44**, 5641–5652.
57 J. Valentin-Reyes, D. B. Trejo, O. Coreno and J. Luis Nava, *Chemosphere*, 2022, **297**, 134144.